

Article

Cry Protein Crystal-Immobilized Metallothioneins for Bioremediation of Heavy Metals from Water

Qian Sun, Sze Wan Cheng, Kelton Cheung, Marianne M. Lee * and Michael K. Chan *

School of Life Sciences and Center of Novel Biomaterials, The Chinese University of Hong Kong, Shatin, New Territories, Hong Kong SAR, China; sunqian@link.cuhk.edu.hk (Q.S.); 1155034893@link.cuhk.edu.hk (S.W.C.); skykelton@gmail.com (K.C.)

* Correspondence: mariannemmlee@cuhk.edu.hk (M.M.L.); michaelkchan88@cuhk.edu.hk (M.K.C.)

Received: 8 May 2019; Accepted: 30 May 2019; Published: 1 June 2019



Abstract: Cry proteins have been the subject of intense research due to their ability to form crystals naturally in *Bacillus thuringiensis* (*Bt*). In this research we developed a new strategy that allows for the removal of cadmium and chromium from wastewater by using one Cry protein, Cry3Aa, as a framework to immobilize tandem repeats of the cyanobacterial metallothionein SmtA from *Synechococcus elongatus* (strain PCC 7942). SmtA is a low molecular weight cysteine-rich protein known to bind heavy metals. A series of Cry3Aa-SmtA constructs were produced by the fusion of one, three, or six tandem repeats of SmtA to Cry3Aa. Overexpression of these constructs in *Bt* resulted in the production of pure Cry3Aa-SmtA fusion crystals that exhibited similar size, crystallinity, and morphology to that of native Cry3Aa protein crystals. All three Cry3Aa-SmtA constructs exhibited efficient binding to cadmium and chromium, with the binding capacity correlated with increasing SmtA copy number. These results suggest the potential use of Cry3Aa-SmtA crystals as a novel biodegradable and cost-effective approach to the removal of toxic heavy metals from the environment.

Keywords: Cry protein crystals; metallothioneins; bioremediation; heavy metal contamination

1. Introduction

Cry proteins are a family of proteins that are produced and directly crystallized within the bacterium *Bacillus thuringiensis* (*Bt*) [1–4]. The resulting crystals are very stable and can be isolated with minimal purification. In many cases, simple washing is all that is needed to remove soluble impurities. Functionally, Cry proteins are most famous for their role as biological insecticides. They have been incorporated into many genetically modified crops as a way to make the crops resistant to insect and nematode pests [5]. Due to their use in genetically modified crops that are consumed by humans, Cry proteins are generally considered to be safe for organisms [6]. Our group was the first to demonstrate that various reporter proteins could be fused to one such Cry protein, Cry3Aa, to produce isolatable Cry3Aa fusion crystals without apparent loss of reporter function. Isolated Cry3Aa-GFP or Cry3Aa-mCherry crystals were fluorescent, indicating the proper folding of GFP and mCherry, while Cry3A-luciferase crystals remained functionally active and could be used for in vivo imaging studies in mice [7]. It should be noted that while the crystalline nature of some Cry protein crystals produced in *Bt* has been confirmed by powder diffraction [8], and in the case of Cry3Aa, its structure determination [4], we have not been able to use diffraction to confirm this for our Cry3Aa fusions. Nevertheless, their morphology, uniformity, and insolubility are similar to those of native Cry3Aa crystals, and as such, we loosely use the term crystals to reflect this similarity. Consistent with these properties, we recently demonstrated that the lipase lipA from *Bacillus subtilis* could be immobilized by genetically fusing it to Cry3Aa and the resultant Cry3Aa-lipA fusion crystals were found to be more

stable against temperature and solvent than the free lipA protein, thus enabling multiple cycles of biodiesel conversion [9]. Herein, we extend the application of this Cry3Aa fusion technology for use in heavy metal sequestration.

The release of heavy metals such as cadmium (Cd) or chromium (Cr) into natural water ecosystems has increased with expanding industrialization [10], with industrial wastewater from mining, metal processing, tanneries, pharmaceuticals, pesticides, organic chemicals, rubber and plastics, lumber and wood products being common sources of heavy metal pollutants [11,12]. The exposure of these heavy metals to humans can be harmful, leading to chronic or acute health conditions [13], including reduced growth and development, cancer, organ damage, nervous system damage, and in extreme cases, death [14–16]. Due to the mobility and toxicity of heavy metal ions in water, effective methods for their removal are needed. Several different physicochemical methods such as chemical precipitation and membrane filtration have been utilized for this purpose, but there are disadvantages to each of these methods, including high cost, energy requirement, or production of harmful by-products [17–20].

To produce our biologically inspired immobilized chelator, we chose to genetically fuse Cry3Aa to the metallothionein SmtA from the cyanobacterium *Synechococcus elongatus* (strain PCC 7942). Metallothioneins are low molecular weight cysteine-rich proteins with a high binding capacity for heavy metals due to the presence of multiple cysteine residues that facilitate the formation of metal-thiolate clusters at sub-micromolar concentrations [21–25]. SmtA is arguably the best characterized bacterial metallothionein. The NMR structure of a Zn²⁺-bound SmtA suggests that its cysteine residues form a pocket for binding four metal ions [26]. Like other metallothioneins, this use of cysteines to ligate the metal ions provides SmtA with selectivity towards soft metals such as Hg²⁺, Cd²⁺, Zn²⁺, Cu²⁺, and Co²⁺, allowing it to be used as a metal chelator of toxic heavy metals such as Cd²⁺—even in the presence of high concentrations of sodium, calcium, and magnesium [27,28]. This property makes them potentially useful for multiple purposes [15,29–33], including as binding agents for the selective removal of heavy atoms from contaminated water [27]. Here we describe the *in vivo* production and physical characterization of three different Cry3Aa-SmtA fusion crystals, and the evaluation of their ability to remove Cd²⁺ and Cr³⁺ ions from heavy metal-containing solutions.

2. Materials and Methods

2.1. Construction of the Cry3Aa-SmtA Fusion Plasmids

The gene encoding three tandem repeats of SmtA ([SmtA]₃) was synthesized and cloned into a standard plasmid by GeneArt (ThermoFisher). A single copy of SmtA ([SmtA]) or [SmtA]₃ was amplified by PCR using Kapa HiFi Hot Start Ready Mix (Kapa Biosystems) from the aforementioned plasmid while the gene fragment encoding six repeats of SmtA ([SmtA]₆) was generated by overlap PCR of two [SmtA]₃ fragments. Each gene was subcloned into an existing pHT315 vector harboring the *cry3Aa* gene (pHT315-Cry3Aa) [7]. Briefly, the pHT315-Cry3Aa vector was linearized using the restriction endonucleases BamHI and KpnI, and the gene fragment [smtA]_x was then cloned between the BamHI and KpnI sites downstream of the *cry3Aa* gene using Gibson Assembly® Master Mix (New England Biolabs) following the manufacturer's instructions, yielding the plasmids for *Bt* expression of Cry3Aa-[SmtA], Cry3Aa-[SmtA]₃, or Cry3Aa-[SmtA]₆ protein crystals.

2.2. Expression and Purification of Cry3Aa and Cry3Aa-SmtA Fusion Crystals in *Bt*

All *Bt* Cry3Aa and Cry3Aa-SmtA fusion protein crystals were produced by transforming the corresponding plasmids into *Bt407* cells. The cells were overexpressed at 25 °C for 72 h, after which the pellet was harvested using centrifugation at 8000 rpm for 10 min. The pellet was washed with autoclaved double distilled water (ddH₂O) and purified by centrifugation using a discontinuous sucrose gradient (40% 4 mL, 55% 7 mL, 65% 7 mL, 72% 4 mL) at 5000 rpm for 30 min. The crystals were extracted from the 55% and 65% layer and washed with autoclaved ddH₂O to remove the sucrose. SDS-PAGE samples were prepared by resuspending crystals in autoclaved ddH₂O, adding 5× SDS

dye, boiling for 5 min, and then loading onto a 10% TGX Stain-Free gel (BioRad) to verify the presence and purity of the corresponding crystals. Protein concentrations were determined using the Bradford standard assay (BioRad).

2.3. Dynamic Light Scattering of Cry3Aa and Cry3Aa-SmtA Fusion Crystals

The size and dispersity of Cry3Aa and the three Cry3Aa-SmtA fusion crystals were measured by dynamic light scattering (DLS) at 25 °C by resuspending 100 µg of crystals in 1 mL of autoclaved ddH₂O and then applying them to a Malvern Zetasizer Nano ZS90 (Malvern Instruments Ltd., Malvern, UK).

2.4. Scanning Electron Microscopy of Cry3Aa and Cry3Aa-SmtA Fusion Crystals

Scanning electron microscopy (SEM) imaging samples were prepared by resuspending 0.1 mg of Cry3Aa or Cry3Aa-SmtA fusion crystals in 1 mL autoclaved ddH₂O. The samples were sonicated for 5 min and 2 µL of this solution was added to a copper stub and allowed to dry overnight. Samples were coated with Au using a Sputter Coater S150B (Edwards) and imaged in a SU8000 (Hitachi) operated at 5 kV and a working distance of 8.0 mm to 8.2 mm. The length and width of crystals were measured using software ImageJ Version 1.52a (NIH, Bethesda, MD, USA).

2.5. Metal Binding Capacity Studies by Atomic Absorption Spectrophotometer (AAS)

To ascertain the effect of fusing different numbers of repeat units of SmtA to Cry3Aa on the binding capacity of the corresponding fusion crystals to Cd²⁺ and Cr³⁺ ions, 1 nmol of Cry3Aa (control), Cry3Aa-[SmtA], Cry3Aa-[SmtA]₃, or Cry3Aa-[SmtA]₆ was incubated with 2 mL of 0.1 ppm of Cd standard for AAS (Sigma) or Cr standard for AAS (Sigma) solution at room temperature overnight. The samples were filtered with a 0.22 µm filter and the remaining Cd²⁺ or Cr³⁺ ions in the supernatant were measured by atomic absorption spectrometry (AAS) (Hitachi Z2300 flame). The metal concentrations were determined by comparing the measured absorbance against a series of calibration standards from 0 to 1 ppm prepared from a Cd standard solution (Sigma) or Cr standard solution (Sigma), and then used to derive the % bound by subtracting from the initial amount (0.1 ppm).

2.6. Statistical Analysis

GraphPad Prism software (version 8.0.2, GraphPad, San Diego, CA, USA) was used for statistical analysis. An unpaired two-tailed student's *t*-test was used for size comparison of the Cry3Aa-SmtA fusions with native Cry3Aa. One-way analysis of variance (ANOVA) was used for the multi-group comparison of metal binding by the different constructs. Data are presented as mean ± standard error of the mean.

3. Results

3.1. Production of Cry3Aa and Cry3Aa-SmtA Fusion Crystals

Previous work by our group demonstrated the utility of Cry3Aa as an immobilization platform to generate crystalline particles with functional fusion partners such as green fluorescent protein, mCherry, luciferase, and lipase A [7,9]. To further expand the utility of the Cry3Aa protein crystal platform, we decided to explore whether these crystals could be used to accommodate multiple copies of a small protein, such as a metallothionein, and in so doing, improve their utility—in this case, for increasing metal binding capacity. As such, a series of plasmids containing the gene encoding Cry3Aa-SmtA with different numbers of SmtA repeats were constructed and the corresponding Cry3Aa-SmtA fusion protein crystals were produced in *Bt407*. The identity and purity of each of the Cry3Aa-SmtA fusion crystals were confirmed by SDS-PAGE (Figure 1) based on their molecular weights.

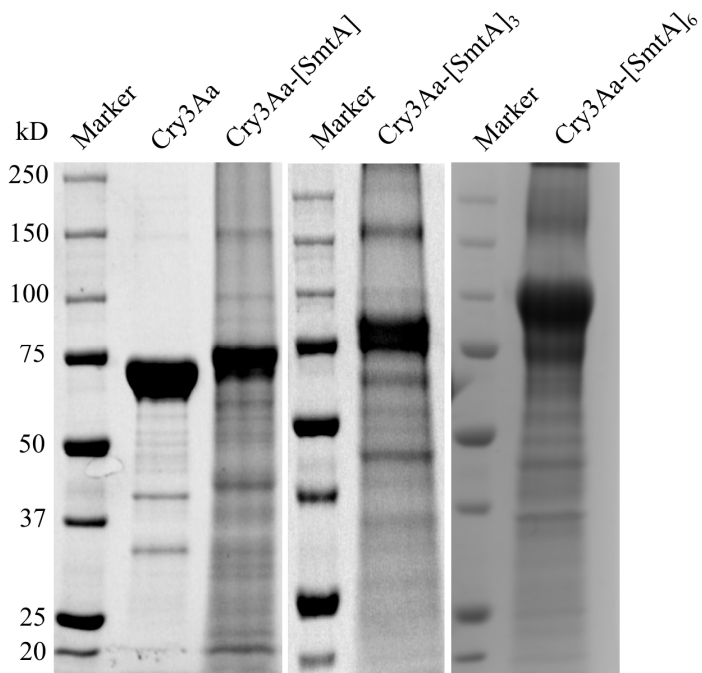


Figure 1. SDS-PAGE of Cry3Aa and Cry3Aa-SmtA fusion crystals produced in *Bacillus thuringiensis* (*Bt*). The theoretical molecular weights are: Cry3Aa, 73.1 kDa; Cry3Aa-[SmtA], 78.8 kDa; Cry3Aa-[SmtA]₃, 90.3 kDa; and Cry3Aa-[SmtA]₆, 107.5 kDa.

3.2. Characterization of Cry3Aa and Cry3Aa-SmtA Fusion Protein Crystals

The size and morphology of each Cry3Aa-SmtA fusion crystal were investigated by DLS and SEM and compared to those of Cry3Aa. Based on the DLS measurements, the size distributions of the different Cry3Aa-SmtA fusion crystals were similar to that of native Cry3Aa crystals (Figure 2a–d). The mean hydrodynamic diameters and polydispersity index (PDI) of Cry3Aa-[SmtA], Cry3Aa-[SmtA]₃, and Cry3Aa-[SmtA]₆ were found to be 860.8 nm (PDI = 0.147), 862.7 nm (PDI = 0.226), and 895.1 nm (PDI = 0.015), respectively, whereas that of the native Cry3Aa was 754.1 nm (PDI = 0.035). In agreement with the DLS results, SEM images of Cry3Aa and the three Cry3Aa-SmtA fusion crystals revealed that the morphologies of the Cry3Aa-SmtA fusion crystals were also similar to that of Cry3Aa crystals (Figure 3a–h)—a rod-like shape of similar length and width (Table 1). These findings suggest that the fusion of SmtA and its repeats to Cry3Aa did not appear to alter the crystal-forming properties of Cry3Aa with respect to both its size and morphology.

Table 1. The mean length and width of Cry3Aa and Cry3Aa-SmtA fusion crystals based on scanning electron microscopy (SEM) images.

Construct	Length (nm) *	Width (nm) *
Cry3Aa	1215 ± 197	912 ± 97
Cry3Aa-[SmtA]	1378 ± 86	871 ± 138
Cry3Aa-[SmtA] ₃	1471 ± 195	1014 ± 151
Cry3Aa-[SmtA] ₆	1405 ± 112	913 ± 48

* Any difference between Cry3Aa-SmtA fusion and Cry3Aa crystals was not statistically significant ($p > 0.05$), as confirmed by unpaired two-tailed student's *t*-test.

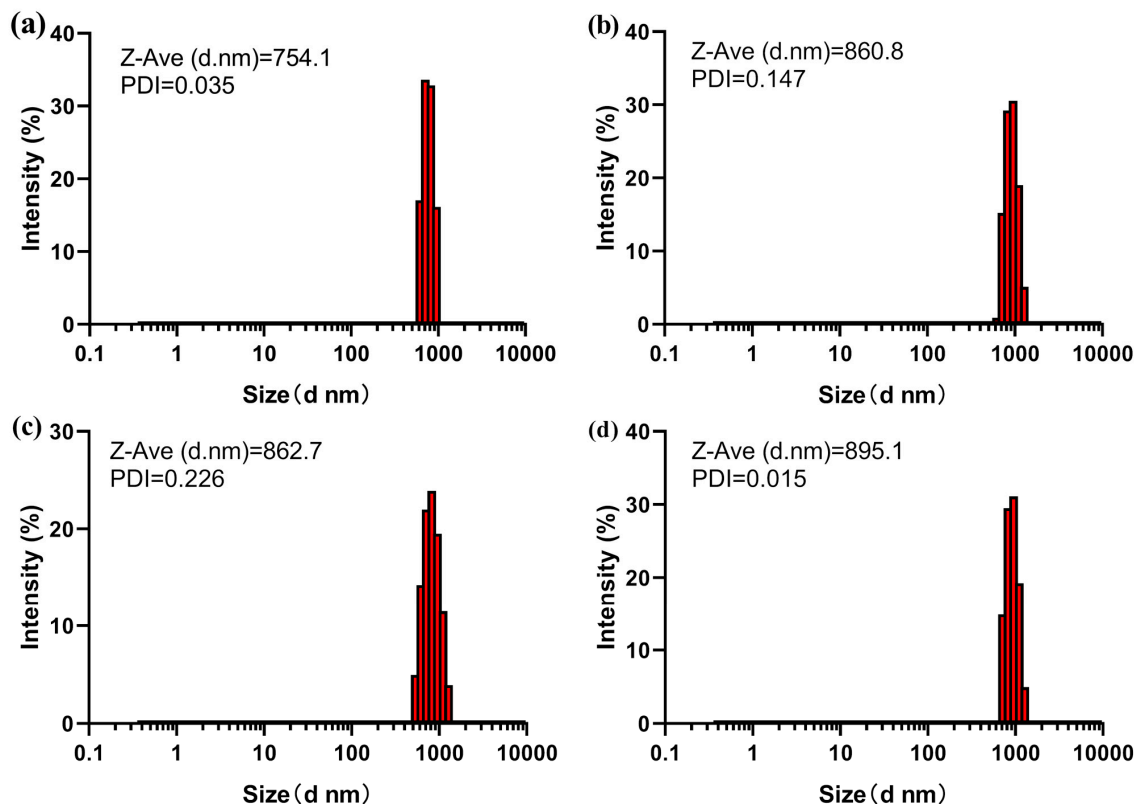


Figure 2. Size comparison of Cry3Aa and Cry3Aa-SmtA fusion crystals by dynamic light scattering (DLS). (a) Cry3Aa, (b) Cry3Aa-[SmtA], (c) Cry3Aa-[SmtA]₃, and (d) Cry3Aa-[SmtA]₆. All samples were measured at a concentration of 100 $\mu\text{g}/\text{mL}$ of crystal.

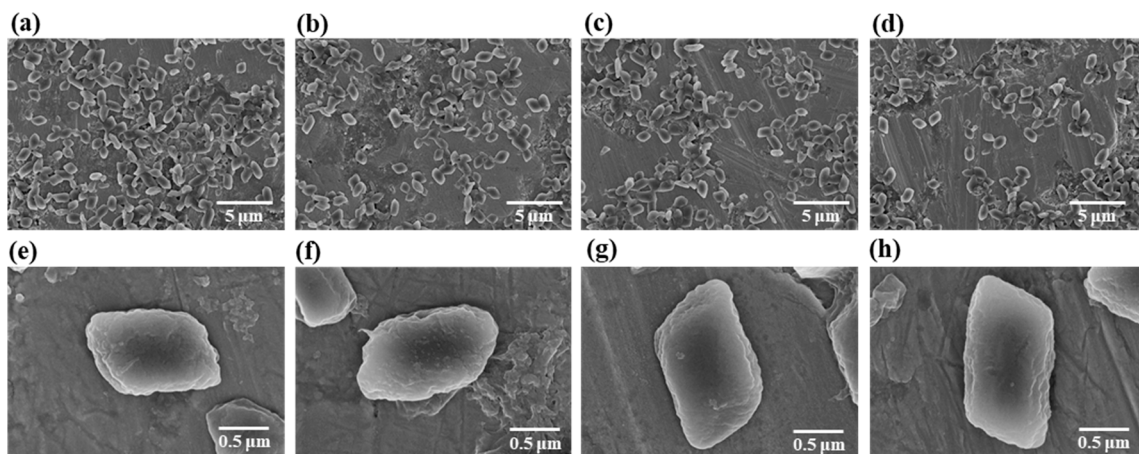


Figure 3. Size and morphological comparison of Cry3Aa and Cry3Aa-SmtA fusion crystals by scanning electron microscopy (SEM). Global SEM images of purified crystals of (a) Cry3Aa, (b) Cry3Aa-[SmtA], (c) Cry3Aa-[SmtA]₃, and (d) Cry3Aa-[SmtA]₆ at 5000 \times magnification. SEM images of single crystals of (e) Cry3Aa, (f) Cry3Aa-[SmtA], (g) Cry3Aa-[SmtA]₃, and (h) Cry3Aa-[SmtA]₆ at 45,000 \times magnification.

3.3. Cadmium and Chromium Binding by Cry3Aa and Cry3Aa-SmtA Fusion Crystals

To evaluate the heavy metal binding capacity of the Cry3Aa-SmtA fusion constructs, 1 nmol each of Cry3Aa-SmtA fusion and Cry3Aa (as a control) crystals were incubated with 2 mL of 0.1 ppm of Cd standard solution or Cr standard solution (Figure 4). As revealed by the AAS assay, Cd binding to the Cry3Aa-SmtA constructs increased with increasing SmtA repeats. Of note, Cry3Aa-[SmtA]₆ crystals bound nearly 100% of the Cd²⁺ ions in 0.1 ppm solution, suggesting that these fusion crystals were

able to remove Cd²⁺ ions even at trace levels (Figure 4a). Similar trends were also observed for binding of Cr³⁺ ions, with the Cry3Aa-[SmtA]₆ crystals showing the highest level of Cr binding (Figure 4b).

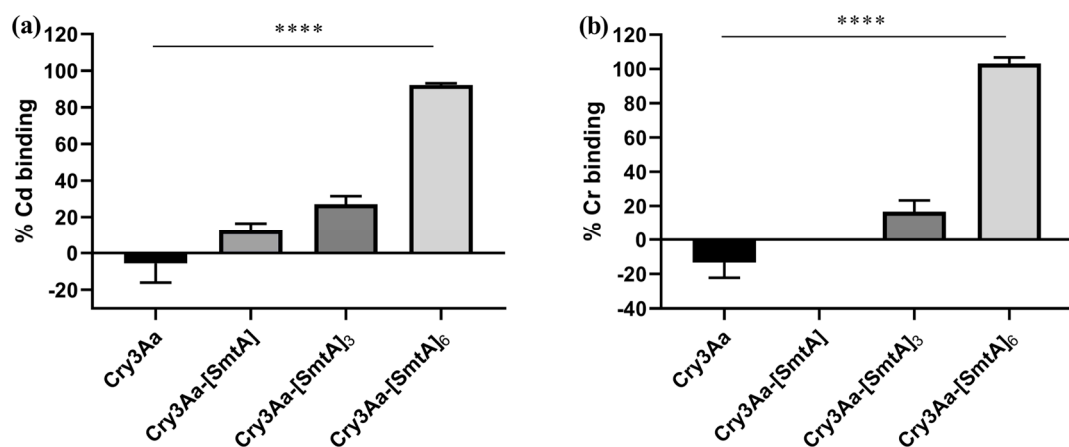


Figure 4. Atomic absorption spectrometry (AAS) analysis of the metal binding capacity of Cry3Aa (control) and Cry3Aa-SmtA fusion crystals. Percentage of (a) Cd²⁺ and (b) Cr³⁺ ions bound to crystals. All measurements were performed in triplicate. The error bars show the standard deviation of the mean. Repeated measurements of Cry3Aa-[SmtA] showed no binding of Cr³⁺ ions. *** $p < 0.0001$ by one-way ANOVA.

4. Discussion

There has been long-term interest in developing metallothioneins for use in the selective removal of heavy metals from wastewater [27]. Their selectivity allows for the binding of toxic metal ions such as Cd²⁺ or Cr³⁺ without removing other metal ions that might be important for the environment [28]. A major challenge, however, is the generation of an immobilized metallothionein for this purpose in a cheap and easy fashion that allows for its potential recycling.

As demonstrated here, the Cry3Aa crystal as an immobilization platform is particularly attractive for this purpose. A plasmid for the expression of Cry3Aa fused to tandem repeats of the SmtA can be readily produced and used for the production of Cry3Aa-SmtA fusion crystals directly in *Bt*. These crystalline particles can easily be purified without the use of columns by density gradient centrifugation, greatly simplifying the isolation step and lowering the cost of production.

While the fusion of one SmtA to Cry3Aa gives only limited binding of heavy metals, we show that up to six tandem repeats of SmtA can be incorporated, resulting in enhanced metal binding without significantly changing the size and morphology of the biologically produced crystal. As an aside, the Cry3Aa-[SmtA]₉ construct with nine copies of SmtA was also cloned, but the yields were low and the resultant crystalline particles seemed less stable. This may suggest that the solvent channels within Cry3Aa crystals can accommodate six copies of SmtA, but not nine. Increasing the number of copies of SmtA is important for metal binding; however, the metal binding capacity for either Cd²⁺ or Cr³⁺ is strongly correlated with the number of SmtA repeats incorporated. The results affirm the potential use of biologically produced Cry3Aa-SmtA fusion crystals for the bioremediation of heavy metals from wastewater.

While there are a number of conventional treatment processes such as ion exchange, activated charcoal, chemical precipitation, and chemical reduction and adsorption, these approaches have certain limitations including their high cost, production of secondary waste, and limited effectiveness at low concentrations of metal [34,35]. In contrast, Cry3Aa-SmtA fusion crystals can be produced directly in bacteria, are easy to isolate, and for the Cry3Aa fusion construct with six copies of SmtA, Cry3Aa-[SmtA]₆ can efficiently remove Cd²⁺ or Cr³⁺ ions from solutions even at trace levels of 0.1 ppm. Thus, Cry3Aa-SmtA fusion protein crystals offer an environmentally friendly, effective, and

economical alternative method for the removal of heavy metals from water—highlighting yet another use of biologically produced Cry3Aa fusion crystals for practical application.

Author Contributions: Conceptualization, M.K.C. and M.M.L.; investigation, Q.S., S.W.C., K.C.; writing—original draft preparation, Q.S., M.K.C. and M.M.L.; supervision, M.K.C. and M.M.L.; funding acquisition M.K.C. and M.M.L.

Funding: This research was funded by the Hong Kong Research Grants Council GRF grant 14300414 and the Center of Novel Biomaterials, the Chinese University of Hong Kong.

Acknowledgments: We would like to thank Josie Lai (CUHK SBS) for her assistance in collecting the SEM images, and Didier Lereclus (Institut Pasteur in Paris) and Daniel Ziegler (*Bacillus* Genetic Stock Center, Ohio State University, USA) for kindly providing us with the *Bt* cells.

Conflicts of Interest: The authors declare no conflict of interest.

References

- Whiteley, H.R.; Schnepf, H.E. The Molecular Biology of Parasporal Crystal Body Formation in *Bacillus thuringiensis*. *Annu. Rev. Microbiol.* **1986**, *40*, 549–576. [[CrossRef](#)] [[PubMed](#)]
- Schnepf, E.; Crickmore, N.; Van Rie, J.; Lereclus, D.; Baum, J.; Feitelson, J.; Zeigler, D.R.; Dean, D.H. *Bacillus thuringiensis* and Its Pesticidal Crystal Proteins. *Microbiol. Mol. Biol. Rev.* **1998**, *62*, 775–806.
- Park, H.-W.; Ge, B.; Bauer, L.S.; Federici, B.A. Optimization of Cry3A Yields in *Bacillus thuringiensis* by Use of Sporulation-Dependent Promoters in Combination with the STAB-SD mRNA Sequence. *Appl. Environ. Microbiol.* **1998**, *64*, 3932–3938. [[PubMed](#)]
- Sawaya, M.R.; Cascio, D.; Gingery, M.; Rodriguez, J.; Goldschmidt, L.; Colletier, J.-P.; Messerschmidt, M.M.; Boutet, S.; Koglin, J.E.; Williams, G.J. Protein crystal structure obtained at 2.9 Å resolution from injecting bacterial cells into an X-ray free-electron laser beam. *Proc. Natl. Acad. Sci. USA* **2014**, *111*, 12769–12774. [[CrossRef](#)]
- Shimada, N.; Miyamoto, K.; Kanda, K.; Murata, H. *Bacillus thuringiensis* insecticidal Cry1Ab toxin does not affect the membrane integrity of the mammalian intestinal epithelial cells: An *in vitro* study. *In Vitro Cell. Dev. Biol.-Anim.* **2006**, *42*, 45–49. [[CrossRef](#)] [[PubMed](#)]
- Chowdhury, E.H.; Shimada, N.; Murata, H.; Mikami, O.; Sultana, P.; Miyazaki, S.; Yoshioka, M.; Yamanaka, N.; Hirai, N.; Nakajima, Y. Detection of Cry1Ab protein in gastrointestinal contents but not visceral organs of genetically modified Bt11-fed calves. *Vet. Hum. Toxicol.* **2003**, *45*, 72–75. [[PubMed](#)]
- Nair, M.S.; Lee, M.M.; Bonnagarde-Bernard, A.; Wallace, J.A.; Dean, D.H.; Ostrowski, M.C.; Burry, R.W.; Boyaka, P.N.; Chan, M.K. Cry Protein Crystals: A Novel Platform for Protein Delivery. *PLoS ONE* **2015**, *10*, e0127669. [[CrossRef](#)]
- Holmes, K.; Monro, R.; Holmes, K. Studies on the structure of parasporal inclusions from *Bacillus thuringiensis*. *J. Mol. Biol.* **1965**, *14*, 572–IN25. [[CrossRef](#)]
- Heater, B.S.; Lee, M.M.; Chan, M.K. Direct production of a genetically-encoded immobilized biodiesel catalyst. *Sci. Rep.* **2018**, *8*, 12783. [[CrossRef](#)] [[PubMed](#)]
- George, S.G.; Carpene, E.; Coombs, T.L.; Overnell, J.; Youngson, A. Characterisation of cadmium-binding proteins from mussels, *Mytilus edulis* (L), exposed to cadmium. *Biochim. Biophys. Acta (BBA)-Protein Struct.* **1979**, *580*, 225–233. [[CrossRef](#)]
- Lakherwal, D. Adsorption of heavy metals: A review. *Int. J. Environ. Res. Dev.* **2014**, *4*, 41–48.
- Srivastava, N.; Majumder, C. Novel biofiltration methods for the treatment of heavy metals from industrial wastewater. *J. Hazard. Mater.* **2008**, *151*, 1–8. [[CrossRef](#)] [[PubMed](#)]
- Chowdhury, S.; Mazumder, M.J.; Al-Attas, O.; Husain, T. Heavy metals in drinking water: Occurrences, implications, and future needs in developing countries. *Sci. Total Environ.* **2016**, *569*, 476–488. [[CrossRef](#)] [[PubMed](#)]
- Bailey, S.E.; Olin, T.J.; Bricka, R.; Adrian, D. A review of potentially low-cost sorbents for heavy metals. *Water Res.* **1999**, *33*, 2469–2479. [[CrossRef](#)]
- Demirbaş, A. Heavy metal adsorption onto agro-based waste materials: A review. *J. Hazard. Mater.* **2008**, *157*, 220–229. [[CrossRef](#)]
- Barakat, M. New trends in removing heavy metals from industrial wastewater. *Arab. J. Chem.* **2011**, *4*, 361–377. [[CrossRef](#)]

17. Roy, D.; Greenlaw, P.N.; Shane, B.S. Adsorption of heavy metals by green algae and ground rice hulls. *J. Environ. Sci. Health Part A Environ. Sci. Eng. Toxicol.* **2008**, *28*, 37–50. [[CrossRef](#)]
18. Pansini, M.; Colella, C.; De Gennaro, M. Chromium removal from water by ion exchange using zeolite. *Desalination* **1991**, *83*, 145–157. [[CrossRef](#)]
19. Pérez-Candela, M.; Martín-Martínez, J.; Torregrosa-Maciá, R. Chromium(VI) removal with activated carbons. *Water Res.* **1995**, *29*, 2174–2180. [[CrossRef](#)]
20. Rengaraj, S.; Yeon, K.-H.; Moon, S.-H. Removal of chromium from water and wastewater by ion exchange resins. *J. Hazard. Mater.* **2001**, *87*, 273–287. [[CrossRef](#)]
21. Vašák, M. Advances in metallothionein structure and functions. *J. Trace Elem. Med. Biol.* **2005**, *19*, 13–17. [[CrossRef](#)]
22. Romero-Isart, N.; Vašák, M. Advances in the structure and chemistry of metallothioneins. *J. Inorg. Biochem.* **2002**, *88*, 388–396. [[CrossRef](#)]
23. Blindauer, C.A. Bacterial metallothioneins: Past, present, and questions for the future. *JBIC J. Boil. Inorg. Chem.* **2011**, *16*, 1011–1024. [[CrossRef](#)]
24. Capdevila, M.; Atrian, S. Metallothionein protein evolution: A miniassay. *JBIC J. Boil. Inorg. Chem.* **2011**, *16*, 977–989. [[CrossRef](#)] [[PubMed](#)]
25. Capdevila, M.; Bofill, R.; Palacios, Ò.; Atrian, S. State-of-the-art of metallothioneins at the beginning of the 21st century. *Coord. Chem. Rev.* **2012**, *256*, 46–62. [[CrossRef](#)]
26. Blindauer, C.A.; Harrison, M.D.; Parkinson, J.A.; Robinson, A.K.; Cavet, J.S.; Robinson, N.J.; Sadler, P.J. A metallothionein containing a zinc finger within a four-metal cluster protects a bacterium from zinc toxicity. *Proc. Natl. Acad. Sci. USA* **2001**, *98*, 9593–9598. [[CrossRef](#)] [[PubMed](#)]
27. Esser-Kahn, A.P.; Iavarone, A.T.; Francis, M.B. Metallothionein-Cross-Linked Hydrogels for the Selective Removal of Heavy Metals from Water. *J. Am. Chem. Soc.* **2008**, *130*, 15820–15822. [[CrossRef](#)] [[PubMed](#)]
28. Freisinger, E.; Vašák, M. Cadmium in metallothioneins. In *Cadmium: From Toxicity to Essentiality*; Sigel, A., Sigel, H., Sigel, R.K., Eds.; Springer: Dordrecht, The Netherlands, 2013; Volume 11, pp. 339–371.
29. Verma, N.; Singh, M. Biosensors for heavy metals. *BioMetals* **2005**, *18*, 121–129. [[CrossRef](#)] [[PubMed](#)]
30. Martín-Betancor, K.; Rodea-Palomares, I.; Muñoz-Martín, M.A.; Leganés, F.; Fernández-Piñas, F.; Palomares, I.M.R. Construction of a self-luminescent cyanobacterial bioreporter that detects a broad range of bioavailable heavy metals in aquatic environments. *Front. Microbiol.* **2015**, *6*, 186. [[CrossRef](#)] [[PubMed](#)]
31. Bontidean, I.; Berggren, C.; Johansson, G.; Csöregi, E.; Mattiasson, B.; Lloyd, J.R.; Jakeman, K.J.; Brown, N.L. Detection of Heavy Metal Ions at Femtomolar Levels Using Protein-Based Biosensors. *Anal. Chem.* **1998**, *70*, 4162–4169. [[CrossRef](#)]
32. Wu, C.-M.; Lin, L.-Y. Immobilization of metallothionein as a sensitive biosensor chip for the detection of metal ions by surface plasmon resonance. *Biosens. Bioelectron.* **2004**, *20*, 864–871. [[CrossRef](#)] [[PubMed](#)]
33. Gonzalezbellavista, A.; Atrian, S.; Muñoz, M.; Capdevila, M.; Fàbregas, E. Novel potentiometric sensors based on polysulfone immobilized metallothioneins as metal-ionophores. *Talanta* **2009**, *77*, 1528–1533. [[CrossRef](#)]
34. Lim, A.P.; Aris, A.Z. A review on economically adsorbents on heavy metals removal in water and wastewater. *Rev. Environ. Sci. Bio/Technol.* **2013**, *13*, 163–181. [[CrossRef](#)]
35. Babel, S. Low-cost adsorbents for heavy metals uptake from contaminated water: A review. *J. Hazard. Mater.* **2003**, *97*, 219–243. [[CrossRef](#)]



© 2019 by the authors. Licensee MDPI, Basel, Switzerland. This article is an open access article distributed under the terms and conditions of the Creative Commons Attribution (CC BY) license (<http://creativecommons.org/licenses/by/4.0/>).